Journal of Thermal Science and Engineering Applications,
Volume 15, Issue 3, March 2023, Article number 031014, Paper number TSEA-22-1375
DOI:10.1115/1.4056510

Evaluation of Component Level Degradation in the Boeing 737-800 Air Cycle Machine

Ian Jennions
Integrated Vehicle Health Management Centre
School of Aerospace, Transport & Manufacturing
Cranfield University
Bedfordshire, MK430AL, UK
Email: i.jennions@cranfield.ac.uk

Fakhre Ali[1]
Integrated Vehicle Health Management Centre
School of Aerospace, Transport & Manufacturing
Cranfield University
Bedfordshire, MK430AL, UK
Email: f.ali@cranfield.ac.uk

[1] Corresponding author: f.ali@cranfield.ac.uk

Abstract

An aircraft is composed of several highly integrated and complex systems that enable it to deliver safe and comfortable flight. Its functionality is therefore strongly dependent on the safe operation of these systems within their designed optimal efficiencies. The air cycle machine (ACM) is a sub-system of the passenger air conditioner (PACK) system, its key function is to enable refrigeration of the air in order to comply with the wide-range of cabin environment requirements for maintaining aircraft safety and passenger comfort. The operation of the ACM is governed by the PACK control system which can mask degradation in its component during operation until severe degradation or failure results. The required maintenance is then both costly and disruptive. The ACM has been reported as one of the most frequently replaced sub-system and has been therefore reported as a major driver of unscheduled maintenance by the operators. This paper aims to investigate the component level degradation in the ACM at various severities and quantify the impact of its performance characteristics and associated interdependencies at PACK system level.

In this paper, Cranfield University's in-house ECS simulation framework called SESAC (Simscape ECS Simulation under All Conditions) has been implemented to evaluate degradation in the ACM components in a representative Boeing 737-800 aircraft PACK model. The fault modes of interest are those highlighted by the operators and correspond to the ACM compressor, turbine and interconnecting mechanical shaft efficiency degradation. Simulation results, in terms of temperature, pressure and mass flow at various degradation severities, are presented and discussed for each component at PACK system level. The acquired results suggest that, for all three fault modes, the PACK controller can compensate for an ACM degradation severity of up to 20%, allowing the PACK to sustain the delivery of the demanded temperature and mass flow. For degradation severity of above 20%, the PACK is able to deliver the demanded temperature with a substantially reduced mass flow. This has a significant impact on the PACK's ability to meet the cabin demand efficiently. The methodology reported and the findings conceived serve as an enabler towards formulating an effective PACK fault diagnostics and condition monitoring solution at system level, and fault reasoning at vehicle level.

Nomenclature

Acronyms

Alt	Altitude (m)
APU	Auxiliary Power Unit
ADS	Air Distribution System
ACM	Air Cycle Machine
AIS	Anti-icing System
B737	Boeing 737
CPCS	Cabin Pressure Control System
CHX	Condenser
CPCS	Cabin Pressure Control System
DS	Degradation Severity (%)
ECS	Environmental Control System
HPWS	High Pressure Water Separator
MRO	Maintenance Repair & Overhaul
N	Rotational Speed
OEM	Original Equipment Manufacturer
PACK	Pressurised Air Conditioner
PV	PACK Valve
PVOP	PACK Valve Outlet Pressure (Pa)
PHX	Primary Heat Exchanger
RPM	Revolutions Per Minute
RAI	Ram Air Inlet
RC	Reference Case
RH	Relative Humidity (%)
RHX	Reheater
SESAC	Simscape ECS Simulation under All Conditions
SHX	Secondary Heat Exchanger
TCV	Temperature Control Valve
V&V	Validation & Verification
WS	Water Separator

Symbols

C_{PR}	Compressor pressure ratio
CMP_i	Compressor inlet
CMP_o	Compressor outlet
$CHX_{h,i}$	Condenser hot inlet
$CHX_{h,o}$	Condenser hot outlet
$CHX_{c,i}$	Condenser cold inlet
$CHX_{c,o}$	Condenser cold outlet
C_p	Heat capacity at constant pressure (J/gK)
DS_t	Degradation Severity Turbine (%)
DS_c	Degradation Severity Turbine (%)
DS_m	Degradation Severity mechanical shaft (%)

N_c	Compressor rpm
N_t	Turbine rpm
$\dot{m}$	Mass flow (kg/s)
$\dot{m}_c$	Compressor mass flow (kg/s)
$\dot{m}_t$	Turbine mass flow (kg/s)
$\dot{\mathrm{m}}_{cold}$	mass flow through the PACK ACM (kg/s)
$\dot{\mathrm{m}}_{hot}$	mass flow through the TCV(kg/s)
$\dot{m}_h$	Hot mass flow (kg/s)
$\dot{\mathrm{m}}_{engine}$	mass flow (bleed flow) through the PV (kg/s)
P	Pressure (kPa)
P_{BAS}	Bleed air pressure (kPa)
P_{Cab}	Cabin Pressure (kPa)
PV_i	PACK valve inlet
PV_o	PACK valve outlet
$PHX_{h,i}$	Primary heat exchanger hot inlet
$PHX_{h,i}$	Primary heat exchanger hot outlet
P_{amb}	Ambient Pressure (kPa)
PCK_o	PACK outlet
PR_c	Pressure ratio compressor
PR_t	Pressure ratio turbine
$RHX_{h,i}$	Reheater hot inlet
$RHX_{h,o}$	Reheater hot outlet
$RHX_{c,i}$	Reheater cold inlet
$RHX_{c,o}$	Reheater cold outlet
$SHX_{h,i}$	Secondary heat exchanger hot inlet
$SHX_{h,o}$	Secondary heat exchanger hot outlet
T_{amb}	Ambient Temperature (K)
T_{target}	PACK outlet target temperature (K)
T_{ci}	Cold side inlet temperature (K)
TRB_i	Turbine inlet
TRB_o	Turbine inlet
T_{co}	Cold side outlet temperature (K)
T_{PR}	Turbine pressure ratio
T_{BAS}	Bleed air temperature (K)
T_{Cab}	Cabin temperature (K)
T_{hot}	TCV flow (bleed) temperature (K)
T_{cold}	Temperature of flow through the ACM (K)
T_{t1}	Turbine inlet temperature (K)
T_{c1}	Compressor inlet temperature (K)
$\dot{W}_c$	Compressor power (W)
$\dot{W}_t$	turbine power (W)
η_t	Turbine isentropic efficiency (%)
η_c	Compressor isentropic effiency (%)
η_m	Shaft mechanical efficiency (%)
γ	Ratio of specific heats $= C_p/C_v$

1. Introduction

1.1 Background

An aircraft is composed of several highly integrated and complex systems that enable it to deliver safe and comfortable flight. Its functionality is therefore strongly dependent on the safe operation of these systems within their designed optimal efficiencies. Maintenance, Repair, and Overhaul (MRO) activities are implemented to retain the functionality of systems, sub-systems, or components that suffer from performance degradation. Maintenance costs are estimated to make up 10% of airline operating costs [1], with spending reported to be around US$83 billion in 2019. Considering the industry efforts to build and recover from the Coronavirus 2019 (COVID19), these costs are anticipated to reach US$115 billion by 2030 [2]. Unscheduled maintenance activities have a substantial impact on these costs. In 2017 alone this amounted to more than US$6.5 billion for wide-body jets and almost US$5 billion for small regional jets due to delays and cancellations [3]. The unscheduled maintenance is significantly more prevalent when considering the legacy aircraft types i.e., Boeing 737 (B737-800) [4]. This has led to a compelling need within the aviation industry to explore innovative aircraft health management solutions that can enable the maintenance of its key systems based on predictive maintenance approaches.

The Environmental Control System (ECS) is one of the major systems of aircraft. ECS is a generic term for the subsystems and equipment associated with ventilation, heating, cooling, contamination control, and pressurization in the occupied compartments, cargo bays, and electronic racks [5]. The key function of the ECS is to enable the aircraft to maintain an environment that ensures the comfort of passengers and crew, as well as to provide adequate cooling to the avionics equipment throughout an aircraft's operational envelope. The overall environmental control system of a typical civil aircraft is composed of several subsystems: the Bleed Air System (BAS), the Anti-Icing System (AIS), the Pressurized Air Conditioner (PACK), and the Cabin Pressure Control System (CPCS). In addition, there are other subsystems such as the ozone converter, the mix manifold, and the Air Distribution System (ADS) which act as intermediaries in an ECS. The detailed operation of each is explained in a greater detail by the authors in [6]. The system of focus in this study is the PACK.

The PACK plays a pivotal role in enabling the ECS to fulfil its functionality, it receives hot and high-pressure air from the bleed air system and conditions it for temperature, pressure, and humidity against the demanded cabin conditions, and supplies it to the cabin through the air distribution system. In an aircraft such as the B737-800, there are two identical PACK systems which are contained in equipment bays located on either side of the aircraft centreline on the underside of the fuselage. The PACK is composed of sub-systems and components: flow and temperature control valves, heat exchanges, a ram air system, water separators and an air cycle machine. The principle component of the PACK is the Air Cycle Machine (ACM), enabling refrigeration through the expansion of the bleed air in order to comply with a wide-range of cabin environment requirements. The PACK is prone to degradation which can lead to the functional failure of the ECS system. Often these degradation modes are masked by the overall ECS control system and can result in unscheduled maintenance [8]. According to [7], the most frequent ECS faults appear in the primary or secondary heat exchangers, the flow and temperature control valves, the ram air door actuator, and the ACM. Furthermore, the ACM has been reported as one of the most frequently replaced sub-system and is therefore one of the key drivers of unscheduled maintenance.

To understand the failure mechanisms and fault modes associated with the PACK at sub-system and component level, the athors have reported in [8, 9] the evaluation of degradation in the PACK heat exchangers, ram air system, flow and temperature control valves, and the development of associated fault diagnostics[10]. In this paper, a further expansion of the research to investigate critical faults associated with the PACK ACM has been carried out. The fault modes of interest are those

highlighted by the operators and correspond to the ACM compressor, turbine and mechanical shaft efficiency degradation. The overall aim of the work is, therefore, to understand the physics and engineering of the PACK at the system and component level, for various ACM degradation scenarios. This can facilitate the formulation of an effective PACK fault diagnostics and condition monitoring solution at the system level and faults reasoning at the vehicle level.

1.2 Description of ECS PACK

Figure 1 illustrates the schematic of a single PACK in the B737-800. It consists of valves, heat exchangers, an ACM and High Pressure Water Separator (HPWS). Following the sequence shown in Fig. 1, the bleed air enters the PACK through the PACK Valve (PV), since the bleed air is at high temperature and pressure, it is conditioned through the PACK to match the cabin demand. The primary cooling takes place in the Primary Heat Exchanger (PHX), and secondary cooling takes place in the Secondary Heal Exchanger (SHX) after the flow is compressed. Cold ram air, which originates from outside the aircraft, flows through the ram air duct and, after being used as a heat sink for PHX and SHX, is deposited back into the aircraft's airstream. The SHX significantly reduces the temperature of the flow, subsequent to which the flow is passed throught the HPWS for humidity treatment, and finally, the air is expanded through a turbine, at the outlet of the turbine, the air temperature can potentially drop below freezing and, if this occurs, part of the bypass hot bleed flow through the TCV is mixed with the flow at the turbine outelet to prevent freezing/ice formation. The mixing of TCV air is controlled to match the PACK outlet temperature against the cabin demand. In references [8, 9] authors have thoroughly reported the functionality of the PACK and its operation under various operating modes, including the control system. The focus of this paper is on the ACM functionality and evaluation of its degradation at the component level.

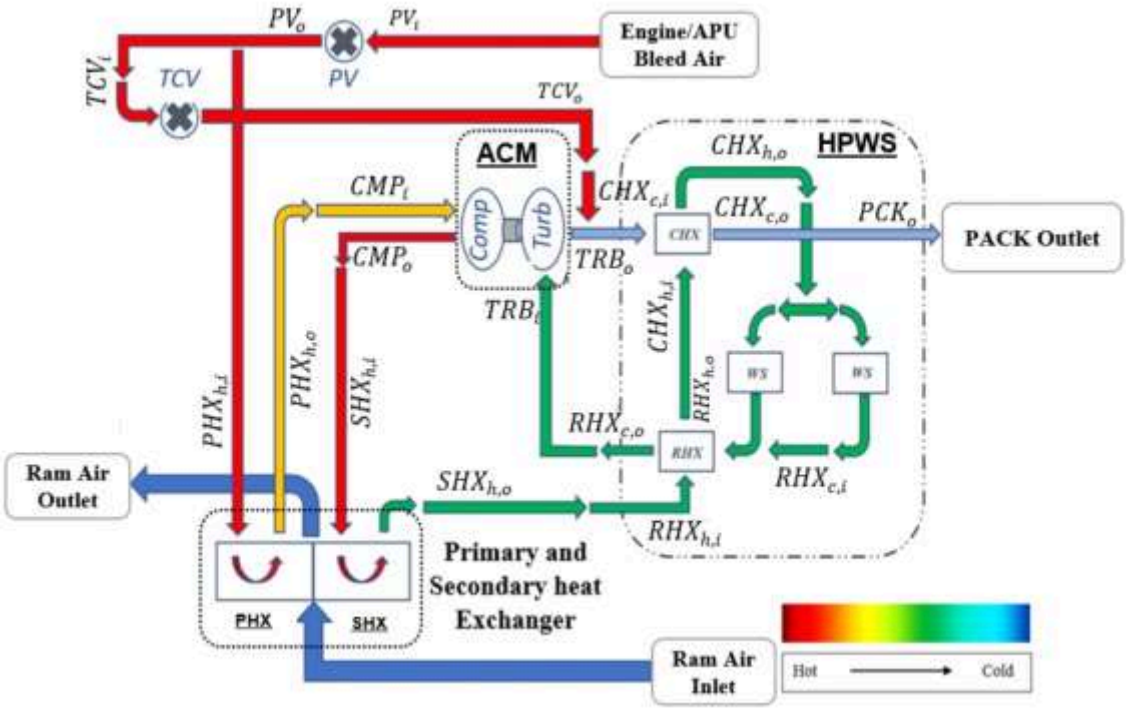

Figure 1: PACK flow schematic and component labelling.

1.3 Description of PACK ACM

The ACM is a sub-system of the PACK and is generally referred to as the cooling unit consisting of a compressor and turbine mounted on a common shaft, as illustrated in Fig. 2. The shaft is bearing mounted in a housing to support the rotating compressor and turbine. The oil sump is formed by the main housing to allow for lubrication of the moving parts. A filler plug and sight gauge are provided

on each side of the housing with a magnetic oil drain plug on the bottom. A duct from the compressor outlet connects to the secondary heat exchanger inlet, which removes the heat added through compression using ram air as a heat sink, after which bleed air is dehumidified by passing through the HPWS.Once the air is dehumidifiedit is fed back into the turbine for expansion. This expansion releases energy to drive the compressor through the interconnecting mechanical shaft. Each PACK is installed with its dedicated ACM. Protection of the ACM is provided by three thermal switches. A compressor discharge overheat switch, turbine inlet overheat switch, and a PACK outlet overheat switch. Actuation of any switch will cause ECS control logic to close the appropriate PACK Valve (PV) and PACK TCV and will illuminate the corresponding PACK amber light on the P5 overhead panel [11]. A detailed description of the PACK protection system in terms of overheat and mass flow control has been reported by the authors in reference [4].

During the operation, the components of the ACM, the compressor, turbine, and the interconnecting shaft can suffer from performance degradation which can potentially lead to PACK functional failure. The primary degradation mechanisms associated with the ACM component failure can stem from a number of sources i.e., shaft frictional losses that can occur in the interconnecting mechanical shaft due to assembly error, lack of lubrication and/or due to fatigue, corrosion, and mechanical damage. These frictional losses can translate into a reduction in the mechanical efficiency of the shaft, which can have a prominent impact on the shaft's ability to transfer the power produced by the turbine to the compressor. The primary source of degradation reported in the compressor and turbine component stem from the mechanisms i.e., fouling, blockage, reduction in tip clearances, and mechanical deformation due to corrosion and fatigue. The degradation in any one of the ACM components can limit the ACM functional performance,which can have a consequent impact on the PACK functional performance, limiting its ability to meet the cabin environmental requirements, and compromising passenger comfort and safety. Furthermore, from the maintenance perspective, degradation in either the compressor or turbine results in the replacement of the entire ACM module, due to its inherent integrated design.

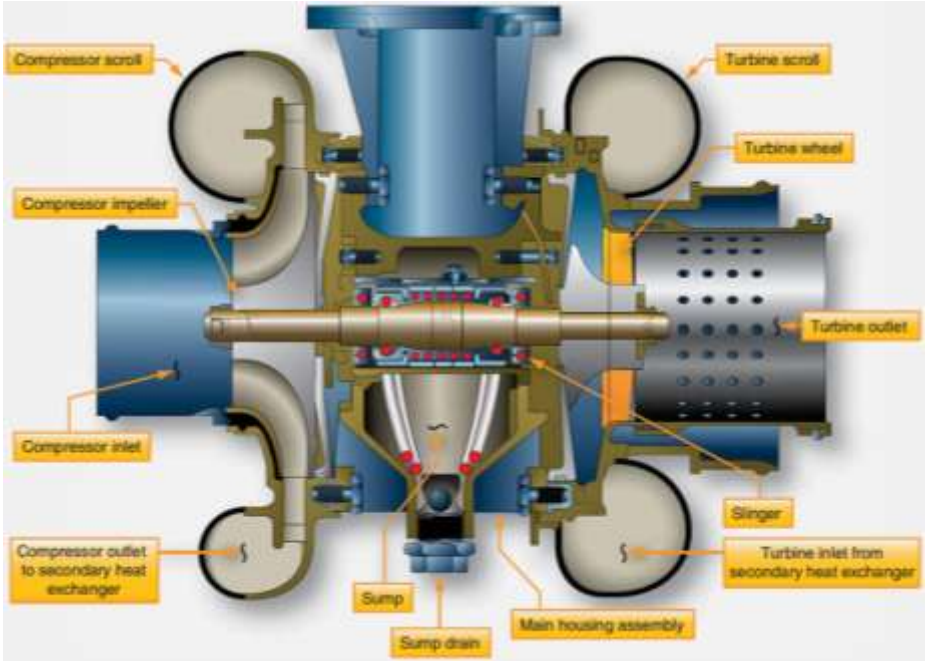

Figure 2: A notional cutaway of an ACM, adopted from [12].

1.4 Existing research on the ACM

There is limited literature dedicated towards the modelling of the ACM performance characteristics in terms of temperature (T), pressure (P), and mass flow ($\dot{m}$) under both healthy and degraded conditions. The reported research primarily focusses on the thermodynamic cycle modelling of the ACM as a standalone system to investigate the impact of changes in the bleed system and cabin parameters on the ACM coefficient of performance [13]. The study reported in [14] utilises a similar approach to investigate the potential of an electrically driven ACM. This paper presents the first study on the simulation of the ACM performance characteristics when subjected to degradation in its components under various severities and quantifies the impact on the PACK performance at the system level.

For modelling the degradation in the ACM compressor and turbine component, relevant information from the literature has been compiled. In terms of the compressor, deformation of the surface and geometry of its blades can change its performance characteristics (i.e. mass flow rate, pressure ratio and isentropic efficiency). As reported in [15], degradation in the compressor typically changes all component characteristics, however, depending on the nature of the degradation, some characteristics might have a stronger change compared to others. For example, increased tip clearance has been reported in [16] to strongly affect all compressor characteristics, while fouling or erosion faults result in a much stronger reduction in the isentropic efficiency compared to the pressure ratio and mass flow, as reported in [18].

With regards to the turbine, like the compressor, faults in this component are generated from changes in its blade surface and geometry. A turbine fault normally affects all turbine characteristics (mass flow rate and efficiency). However, depending on the existing fault mode, one of the turbine characteristics can have a much stronger influence than the other. For example, [19] and [15] report that surface roughness and fouling cause a much stronger reduction in efficiency compared to the mass flow rate. For the purposes of research addressed in this paper, the fault considered in the compressor and turbine emulates a fouling condition as described in [18]. This condition results in a decrease in the isentropic efficiency. The degradation in the interconnecting shaft is modelled based on the reduction in the mechanical efficiency of the shaft caused due to factors such as friction, wear or vibration, assembly error or lubrication issues. The overall formulation of the healthy and degraded performance of the ACM is presented in sections 2.2 and 2.3.

1.5 Scope of present work

Considering the existing literature dedicated to the evaluation of ACM performance characteristics, there exists a gap in understanding of the ACM performance in terms of T, P and $\dot{m}$ under healthy and degraded conditions at the PACK system level. This paper investigates the degradation in the Boeing 737-800 aircraft PACK ACM components at various degradation severities. The discussion of the results focuses on the quantification of the PACK performance characteristics at system level, with specific emphasis on highlighting the interdependencies between various components when exposed to degradation in the ACM. The fault modes of interest are those highlighted by the operators and correspond to the ACM compressor, turbine, and mechanical shaft efficiency degradation. The reported simulation methodology and findings serve as a further step towards the goal of formulating a cost-effective ACM fault isolation and diagnostic solution, as well as supporting fault reasoning at vehicle level.

2 Simulation methodology

2.1 SESAC framework

To support the research addressed in this paper, an ECS simulation framework called SESAC has been used to simulate the PACK degraded performance at sub-system and component levels. SESAC offers a library of modules that can be assembled to model any PACK configuration. It can simulate the health state indicating parameters – T, P, $\dot{m}$ - of the PACK throughout the aircraft operating envelope and under a wide range of functional scenarios. The overall theoretical and computational development of SESAC, as well as its verification and validation, has been thoroughly reported by the authors in reference [6]. Note that the employed B737-800 PACK model in this study mirrors the schematic shown in Fig. 1, and has been reported by the authors in their previous study on the assessment of B737-800 PACK heat exchanger degradation (see Fig. 5, in [8]). The only change that has been made to the model is that the ACM component has been upgraded to incorporate faults in the ACM, with all other components in the system being healthy. To avoid repetition, the PACK model is not reproduced in this paper, the interested reader can access the detailed elaboration of the model from [8].

2.2 Formulation of the ACM

The ACM is responsible for conditioning the high pressure and temperature bleed air supplied to the PACK by the engine compressor or Auxiliary Power Unit (APU). The expansion in the turbine significantly reduces both pressure and temperature of the air, the resul0ting heat energy is converted into mechanical work which is used to drive the compressor through the interconnecting mechanical shaft. In the SESAC model, the formulation of the ACM components is modelled based on the first principles and is assumed to be adiabatic, i.e. no heat exchange between the fluid and the outside environment.

2.2.1 Compressor

For an adiabatic compressor isentropic efficiency is defined as the ratio of the actual work divided by the ideal work as shown below.

$$\eta_c = \frac{isentropic\ work}{actual\ work} = \frac{h_{2i} - h_1}{h_2 - h_1} = \frac{T_{2i} - T_1}{T_2 - T_1} \qquad \text{Eq. 1}$$

$$\frac{T_{2i}}{T_1} = \left(\frac{P_2}{P_1}\right)^{\frac{\gamma-1}{\gamma}} = (PR_c)^{\frac{\gamma-1}{\gamma}} \qquad \text{Eq. 2}$$

The actual outlet temperature and the compressor power can be expressed as follows using the above equations.

$$T_2 = T_1\left\{1 + \frac{1}{\eta_c}\left[(PR_c)^{\frac{\gamma-1}{\gamma}} - 1\right]\right\} \qquad \text{Eq. 3}$$

$$\dot{W}_c = \dot{m}_c C_p (T_2 - T_1) = \frac{\dot{m}_c C_p T_1}{\eta_c}\left[\left(\frac{P_2}{P_1}\right)^{\frac{\gamma-1}{\gamma}} - 1\right] \qquad \text{Eq. 4}$$

The values of the pressure ratio (PR_c) as well as the isentropic efficiency (η_c) come from compressor maps against the mass flow and shaft speed. The maps are proprietary to the Original Equipment Manufacturer (OEM) and therefore cannot be disseminated as part of this study.

2.2.2 Turbine

The formulation of an adiabatic turbine isentropic efficiency accounts for the differences between the ideal and the actual process. This is expressed as the ratio of the actual and ideal work delivered between the same inlet and exit pressures.

$$\eta_t = \frac{isentropic\ work}{actual\ work} = \frac{h_1 - h_2}{h_1 - h_{2i}} = \frac{T_1 - T_2}{T_1 - T_{2i}} \qquad \text{Eq. 5}$$

$$\frac{T_{2i}}{T_1} = \left(\frac{P_2}{P_1}\right)^{\frac{\gamma-1}{\gamma}} = \left(\frac{1}{PR_t}\right)^{\frac{\gamma-1}{\gamma}} \qquad \text{Eq. 6}$$

The outlet temperature and the turbine power can be expressed:

$$T_2 = T_1\left\{1 - \eta_t\left[1 - \left(\frac{P_2}{P_1}\right)^{\frac{\gamma-1}{\gamma}}\right]\right\} \qquad \text{Eq. 7}$$

$$\dot{W}_t = \dot{m}_t C_p (T_1 - T_2) = \dot{m}_t C_p T_1 \eta_t \left[1 - \left(\frac{P_2}{P_1}\right)^{\frac{\gamma-1}{\gamma}}\right] \qquad \text{Eq. 8}$$

In a similar fashion to the compressor, the characteristics such as the pressure ratio and efficiency for a specific operating point are derived through the performance turbine map.

2.2.3 Shaft

The compressor and turbine are both mounted on a common shaft, therefore their rotational speed (N) remains the same (that is $N_t = N_c$) . The expansion through the turbine generates the power that is transferred to the compressor. Note that, the turbine power generated by the turbine is subjected to some losses associated with the shaft. The shaft's mechanical efficiency (η_m) provides a measure of the amount of power that can be transferred to the compressor. Taking the performance parameters of the compressor and turbine, the power balance must satisfy the following expressions:

$$\dot{W}_t = \eta_m \dot{W}_c \qquad \text{Eq. 9}$$

$$\dot{W}_t = \eta_m \dot{W}_c \quad \rightarrow \quad \dot{m}_t C_p T_{t1} \eta_t \left[1 - \left(\frac{1}{PR_t}\right)^{\frac{\gamma-1}{\gamma}}\right] = \eta_m * \left\{\frac{\dot{m}_c C_p T_{c1}}{\eta_c}\left[(PR_c)^{\frac{\gamma-1}{\gamma}} - 1\right]\right\} \qquad \text{Eq. 10}$$

Rotational speed $\qquad N_t = N_c = N \qquad$ Eq. 11

In the simulation model SESAC, the overall ACM components (i.e., compressor, turbine and shaft) have been coded together to represent one dedicated block. This enables the matching procedure of the ACM based on integrated characteristics of bleed air, compressor and turbine performance maps, and shaft equations.

2.3 ACM degradation modes

2.3.1 Degradation of mechanical efficiency

Increase of mechanical losses in the ACM shaft component can stem from factors such as friction, wear or vibration. A malfunction of the shaft can be due to an assembly error or lubrication issues. These losses prevent the compressor from using all the power generated by the turbine.

ACM component includes the option to modify the mechanical efficiency in order to simulate degradation in the ACM shaft, see Eq. 12.

$$\dot{W}_t = (DS_m * \eta_m)\,\dot{W}_c \qquad \text{Eq. 12}$$
$$Where: DS_m = [0: Healthy - 100: fully\ Degrded]$$

2.3.2 Degradation of compressor and turbine efficiency

The ACM compressor and turbine degradation is caused due to fouling of the compressor and turbine blades, resulting in the reduction of their isentropic efficiency. A degradation severity function DS_c and DS_t is introduced in their respective equations, in order to simulate the degradation severity.

$$\dot{W}_c = \dot{m}C_p(T_2 - T_1) = \frac{\dot{m}C_pT_1}{(DS_c * \eta_t)}\left[\left(\frac{P_2}{P_1}\right)^{\frac{\gamma-1}{\gamma}} - 1\right] \qquad \text{Eq. 13}$$

$$\dot{W}_t = \dot{m}C_p(T_1 - T_2) = \dot{m}C_pT_1(DS_t * c_t)\left[1 - \left(\frac{P_2}{P_1}\right)^{\frac{\gamma-1}{\gamma}}\right] \qquad \text{Eq. 14}$$

$$DS_C\ and\ DS_t = [0: Healthy - 100: Fully\ Degraded]$$

2.4 Compilation of reference cases and boundary conditions

In reference [6] the authors have reported the overall development and simulation of the B737-800 model for two Reference Cases (RCs), representing PACK cruise operation at two different altitudes (RC1 - 28000ft and RC2 - 41000ft). The acquired results are corroborated against actual aircraft data in healthy conditions. In consistent with the previous study on heat exchanger degradation, in this paper the RC1 case, shown in Table 1, is adopted as a healthy baseline to assess PACK operation under degraded ACM scenarios. The degradation modes of the PACK ACM are simulated by injecting faults in the ACM components i.e. interconnecting shaft, compressor and turbine. A discussion on the acquired fault simulation results is presented in section 3.

In order to simulate the performance characteristics of the PACK, under given aircraft operating conditions, boundary conditions for the PACK must be defined. These can be categorised in four parts, (i) Aircraft state condition. This allows the model to determine the ram mass flow, which serves as the input to the PHX and SHX cold streams. The ram mass flow is determined based on the aircraft operating conditions, i.e. Mach number, ambient conditions, and ram intake geometry. (ii) Bleed air properties, in terms of P, T, specific humidity, and water content are required. (iii) Target output conditions, i.e. T, P and ṁ. (iv) Component health state, represented by the degradation severity (DS) which varies from 0 (healthy) to 1 (fully degraded).

The readers are directed to the previous study by the authors in which the model boundary conditions have been elaborated (see, section 2.2, in [8]). The only difference between the boundary conditions from the previous study is the inputs to the model for simulating degradation in the ACM components. In the model, the component health state, represented by the degradation severity (DS) which varies from 0 (healthy) to 1 (fully degraded) has been enabled, as presented in section 2.3.

Table 1. Reference Case 1 (RC1) aircraft operating condition

	Alt [ft]	Mach	Tamb [K]	Tamb [C]	Pamb [kPa]
RC 1	28000	0.761	232	-41	33

3 Results and Discussion

This section presents the results acquired based on the simulation of ACM degradation for RC1 under the degradation modes described in Section 2.3. These results are elaborated in terms of T, P and ṁ throughout the PACK at various severities.

3.1 ACM Mechanical Efficiency

Simulation of the healthy baseline case (with degradation severity of 0%) was calibrated with available data and has been reported by the authors in [1]. Figure 3 presents the acquired results in terms of temperature, pressure, and mass flow; an interpretation of these simulation results is given below. Note that the degradation results are shown for up to 70% degradation, representing the maximum possible degradation that could be simulated in the simulation model due to limitations associated with compressor and turbine work balance.

The function of the ACM within the PACK is to provide compression before the SHX, and expansion of the air in the turbine before the merge. The former helps to improve the effectiveness of the SHX, and the latter provides a significant drop in both the pressure and temperature of the air in order to achieve the target temperature. The expansion through the turbine can often lead to temperatures below freezing, therefore hot air flow through the TCV is supplied to the merge to match the target temperature.

At the turbine outlet (see, Fig. 1- TRB_o), the continuity and energy of the system have to be satisfied. Considering that the flow through the TCV is 'hot' and that through the heat exchangers and ACM-turbine is 'cold', these equations are:

$$\dot{m}_{engine} = \dot{m}_{cold} + \dot{m}_{hot} \quad \text{(Eq. 13)}$$

$$\dot{m}_{engine}\, C_p T_{target} = \dot{m}_{cold} C_p T_{cold} + \dot{m}_{hot} C_p T_{hot} \quad \text{(Eq. 14)}$$

In addition, as there can be no pressure discontinuity at the merge, the pressure at the turbine outlet and the TCV outlet are the same.

Note that two control loops are incorporated in the simulation model, one for temperature and the other for mass flow (see Fig. 5 in [8]). The feedback to the controller is provided to each controller through the virtual temperature sensor installed at the turbine outlet (merge) to match the target temperature, and a mass flow sensor at the PACK outlet, which provides a signal to the PV controller to regulate the engine mass flow through the system.

The expansion through the turbine produces power, available to generate compressor work, and is transferred through a common shaft to the compressor. The degradation in the mechanical efficiency translates to an increase in the mechanical losses, which results in a reduction in the amount of available power that can be delivered to the compressor (see Eq. 10). These mechanical losses are predominantly attributed to the increase in shaft overall frictional losses, bearing damage, lack of lubrication, shaft misalignment etc., and consequently has a detrimental impact on the shaft RPM. This consequently results in less power delivered to the compressor.

With the compressor and turbine mounted on the same shaft, the reduction in the RPM (Fig. 4b) has a detrimental impact on the turbine expansion, resulting in warmer outlet temperature (see station TRB_o in Fig. 3a) relative to the healthy baseline. Under these conditions, considering Eq. 14 and the temperatures from Fig. 3(a), T_{target} *and* T_{hot} are known, T_{cold} has marginally increased, due to degradation, so only the mass flow can be redistributed to satisfy energy at the merge. To do this $\dot{m}_{Cold}$ increases, to allow cooler flow through the system, while $\dot{m}_{engine}$ is kept constant. The TCV closes to drop $\dot{m}_{hot}$ and the PV opens to keep $\dot{m}_{engine}$ constant (Fig. 3a), hence $\dot{m}_{cold}$ increases, as

shown in Fig. 3&4(c). The extremely degraded cases, where $\dot{m}_{engine}$ and $\dot{m}_{cold}$ falls will be dealt with later.

The gradual closing of the temperature control valve produces a back pressure that is exerted on the PV, resulting in increasing the PACK valve outlet pressure (Fig. 3b). Since the turbine and compressor are mounted on a common shaft, and the compressor receives the turbine work, with account for degraded shaft mechanical efficiency, the transfer of this work to the compressor reduces with increase in the level of degradation, the compressor pressure ratio is reduced. As the TCV has closed, the compressor cannot pump more to clear this pressure and drive more flow through the cold stream due to the limited available power. As the level of degradation increases there comes a point where the PV angle saturates (fully open 90°º) and cannot deliver any more flow (Fig. 4(a)). At this point (from the results shown in Fig. 3(c), for 30% degradation severity) $\dot{m}_{engine}$ decreases to satisfy the merge conditions, given the PV cannot open further.

It is interesting to note that, for a degradation severity of up to 20% (highlighted in red circles in Fig. 4b), the turbine pressure ratio remains nearly constant, while the compressor pressure ratio significantly drops with the drop in the RPM. The reasons for the former are twofold (i) turbine inlet conditions in terms of temperature and pressure marginally change relative to healthy (Fig. 3a&b), (ii) the increase in $\dot{m}_{cold}$ compensates for the drop in RPM, and the turbine can maintain a near-constant pressure ratio, maintaining the healthy pressure ratio. In the latter case, for the compressor, the TCV imposed back pressure at the PV propagates through the PHX and results in higher compressor inlet pressure relative to the healthy, resulting in the reduction of the pressure ratio across the compressor.

The key observation from the analysis of the ACM mechanical efficiency degradation results is that the PV mass flow controller can compensate for the reduction in the shaft RPM caused due to mechanical losses that constitute a reduction in the mechanical efficiency of up to 20%. The controller is found to maximise (up until saturation) the opening of the PV against the degraded conditions in order to maintain the healthy mass flow throughout the PACK (e.g., the amount of energy supplied to the PACK is retained as healthy). Under these situations, the PACK is able to maintain the outlet flow conditions (i.e., PACK outlet mass flow and temperature remain the same as healthy) despite a degraded ACM. Degradation in mechanical efficiency beyond 20% can have a prominent impact on the PACK's ability to deliver the outlet conditions in terms of the mass flow rate. For example, at 30% degradation, relative to healthy, the mass flow through the PACK ($\dot{m}_{Engine}$) drops by 9.5%, this drop in mass flow is found to significantly increase with increase in the degradation severity, reaching up to 34% at 70% degradation severity. The results suggest that even under severe degradation, the PACK is able to maintain the delivery of the demanded temperature.

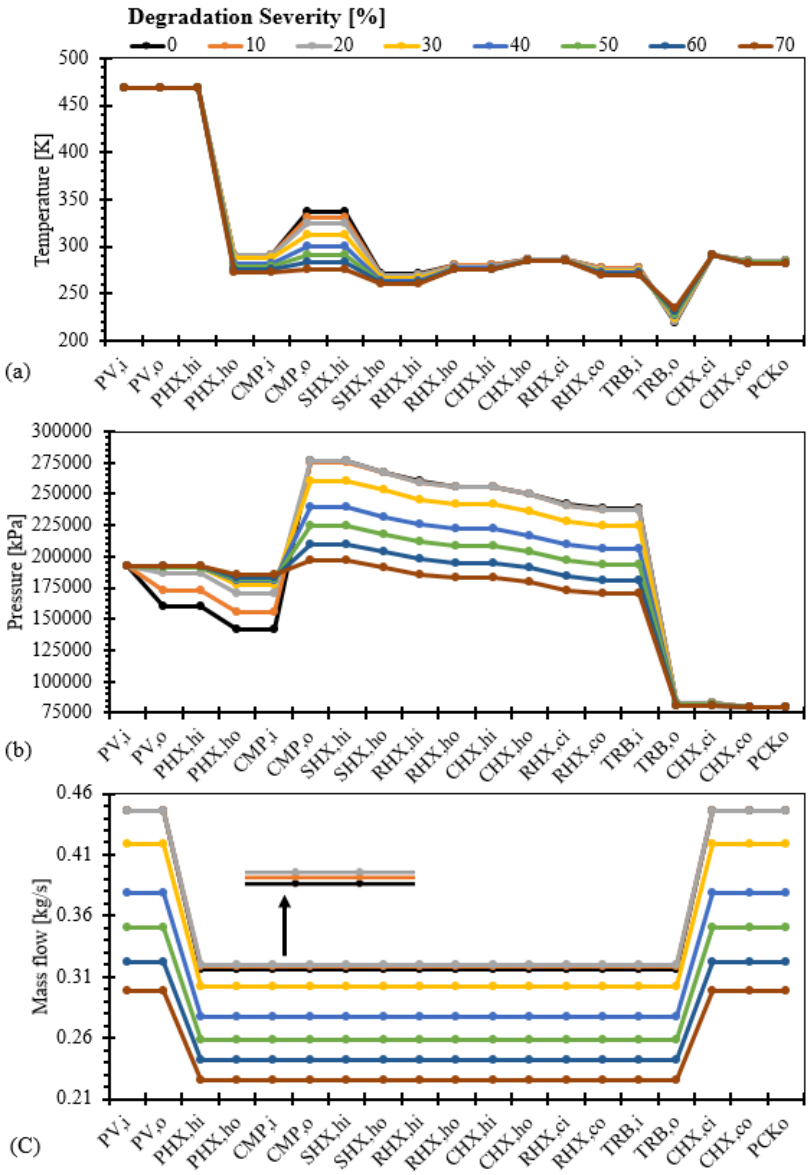

Figure 3: ACM mechanical efficiency degradation results under various severities. 0% represents healthy condition with efficiency value of 80%. Severely degraded case is represented by 70% reduction in the healthy efficiency.

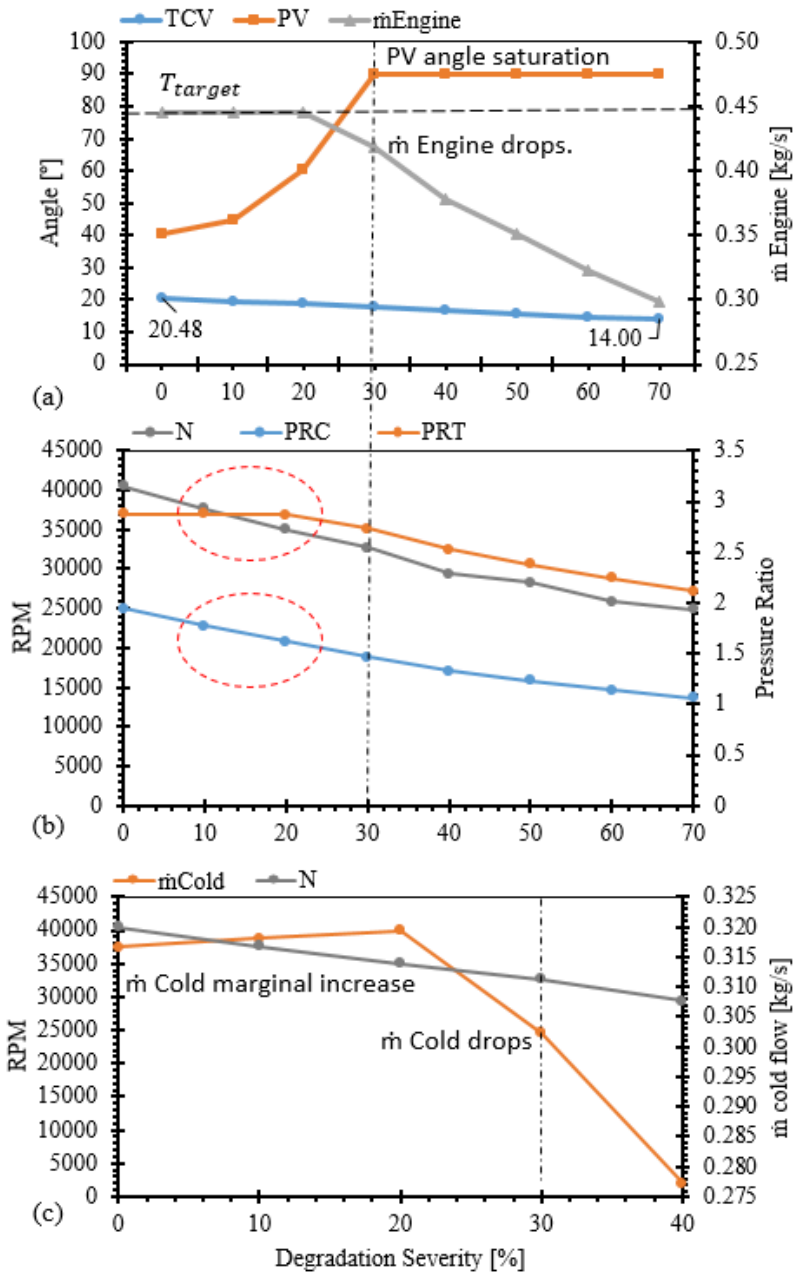

Figure 4: ACM mechanical efficiency degradation results under various severities.

3.2 Compressor Efficiency Degradation

In this section, RC1 is used to simulate the degradation in the compressor efficiency at various severities while the remaining PACK components are in healthy condition. Figure 5 and 6 present the PACK component level performance characteristics in terms of temperature, pressure, mass flow, RPM, and pressure ratio through the compressor and turbine, as well as the PV and TCV valve angles in a similar fashion as presented in the preceding section for mechanical efficiency degradation at various severities.

Analysing the results at the system level, it can be broadly said that the acquired performance results for the compressor efficiency degradation are very similar to the results acquired for the mechanical efficiency degradation. That is, the PACK behaviour in terms of engineering and physics principles is almost identical to the results observed for mechanical efficiency degradation.

As elaborated in section 4.3, compressor modelling is carried out through the matching procedure of the ACM based on bleed air characteristics, compressor performance maps, turbine performance maps and shaft equations in which compressor and turbine rotational speed and powers

are correlated. The degradation in the compressor efficiency causes a change in the operating point of the ACM that imposes the ACM to operate at a reduced RPM relative to the healthy case. And, since the compressor and turbine are mounted on the same shaft, this has an impact on the turbine performance, and the result is a warmer turbine outlet temperature relative to healthy, which demands the TCV to gradually close with the increase in the severity level. The closure of the TCV imposes a back pressure at the PV_O against which the PV controller increases the PV opening in order to maintain the mass flow through the PV until the PV is saturated which occurs at 30% degradation severity (Fig. 5a). At this point the PACK is unable to maintain the mass flow at healthy value. The mass flow through the PV ($\dot{m}_{Engine}$) reduces by 3.4% and is found to significantly increase with the increase in the degradation severity, reaching up to a drop of 36% at 90% severity. Ultimately, the impact of the compressor degradation on the PACK performance characteristics, therefore, remains the same as observed in the case of mechanical efficiency degradation. The PACK can deliver the demanded temperature, however, is unable to maintain the outlet mass flow beyond a given degradation severity (i.e., 20%). From the fault diagnostics point of view, there is no underlying difference in both the faults analysed so far.

Analysing the results at the component level, the results remain the same as observed in the case of mechanical efficiency degradation, except at the compressor outlet. With the increase in the level of severity, the compressor outlet temperature under the mechanical efficiency degradation drops significantly relative to the healthy, and at high severity, there is only a marginal change in the temperature through the compressor (e.g., work done by the compressor is marginal). This is not found to be the case under compressor efficiency degradation, as can be observed from Fig. 5a. Even under high degradation, the compressor is able to perform compression and a noticeable temperature rise is apparent. The reason why this difference occurs between both degradation modes stems from the fact that under mechanical efficiency degradation due to losses in the shaft, the compressor is unable to capitalise the power generated by the turbine to perform work, whereas in the case of compressor efficiency degradation, despite of high degradation in the efficiency the compressor is able to produce work by exploiting the power generated by the turbine.

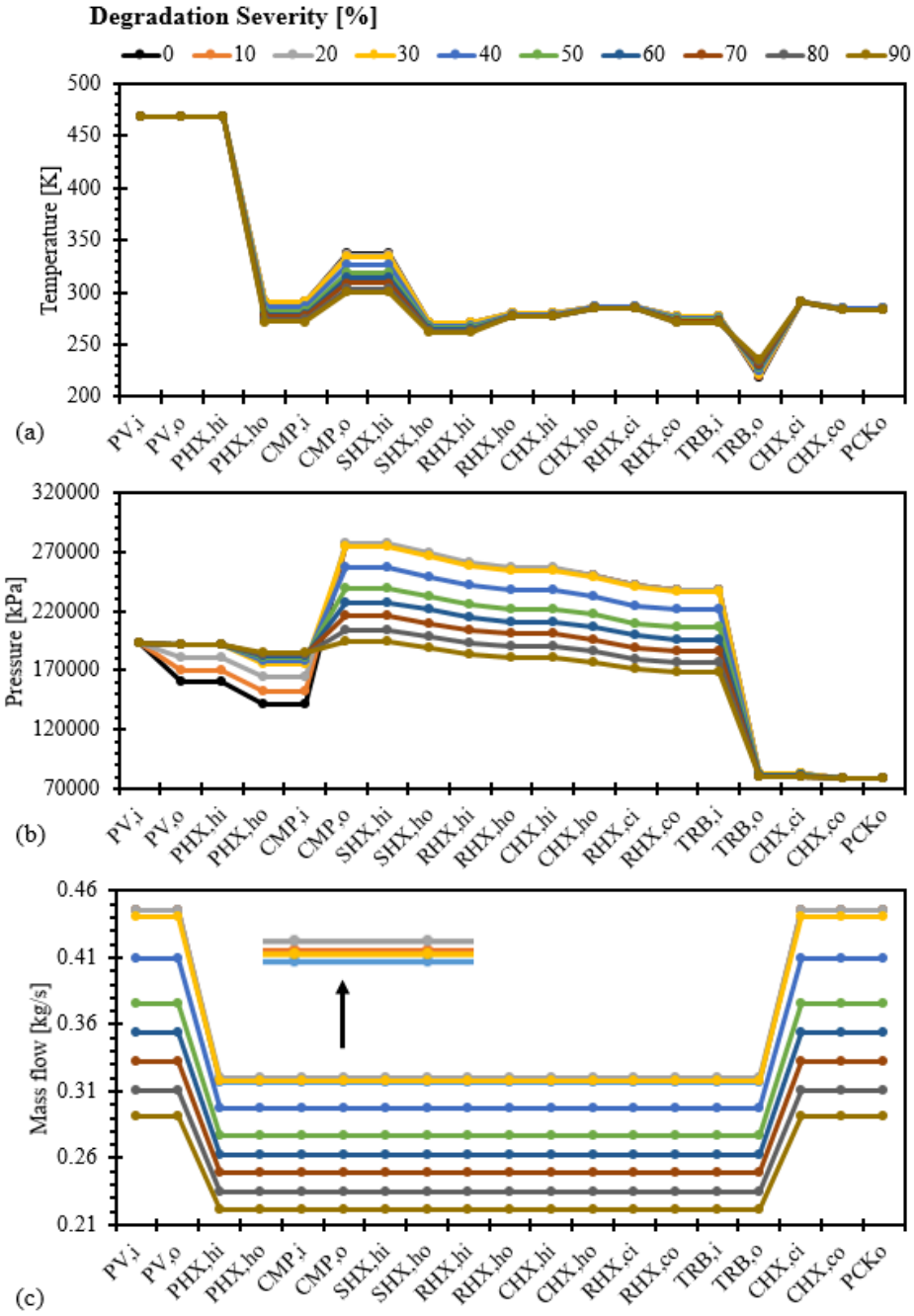

Figure 5: Compressor efficiency degradation results under various severities. 0% represents healthy, and severely degraded case is represented by 90% reduction in the healthy efficiency.

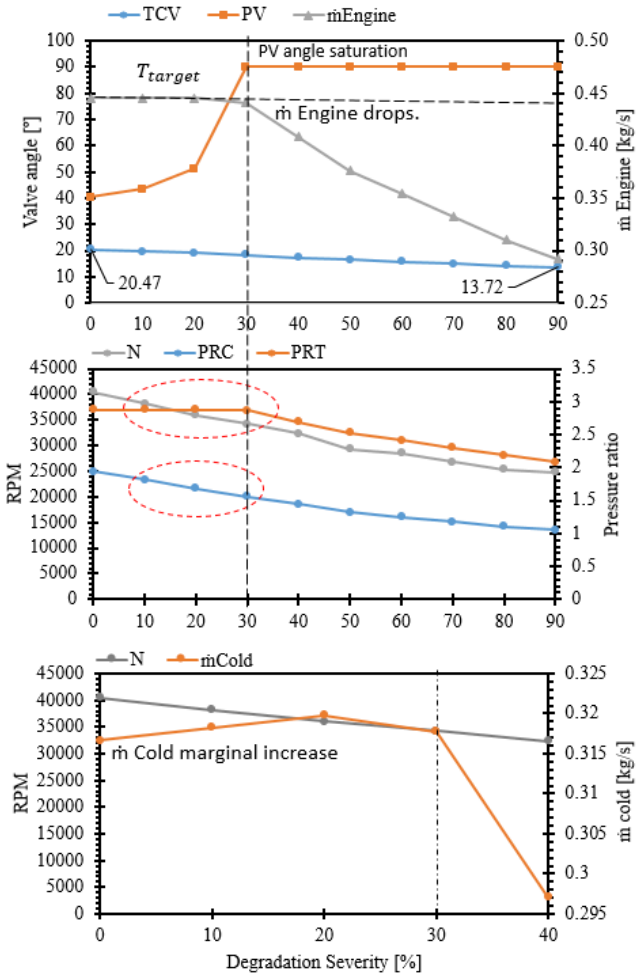

Figure 6: Compressor efficiency degradation results under various severities.

3.3 Turbine Efficiency Degradation

In this section, the simulation results acquired for the turbine efficiency degradation are presented.. Figure 7 and 8 show the PACK component level performance characteristics in terms of temperature, pressure, mass flow, RPM, and pressure ratio through the compressor and turbine, as well as the PV and TCV valve angles for turbine efficiency degradation at various severities.

Analysing the overall PACK performance results presented in Fig. 7 and 8, it can be established that, at the system level, there is no underlying difference between how the PACK responds compared to the degradation cases already presented in the preceding sections. With the degradation in the turbine efficiency, the amount of expansion through the turbine reduces relative to healthy which results in a warmer outlet temperature. This demands the TCV to gradually close with an increase in the level of degradation. The closure of the TCV imposes a back pressure at PV against which the PV controller maximises its opening to maintain the mass flow at a healthy value through the PV. The PV saturates at 30% degradation, as observed in previous cases, and the mass flow through the PV drops. Overall, at the system level, the impact of turbine efficiency degradation on the PACK performance characteristics remains the same as already pointed out in the case of mechanical and compressor efficiency degradation. The PACK is able to deliver the demanded temperature, however, is unable to maintain the outlet mass flow beyond a given degradation severity (i.e. 20%). From a fault diagnostics point of view, therefore there is no underlying difference between all three ACM faults presented. This is an important insight from the condition monitoring and diagnostics point of view, as the parameter that would indicate the health status of the ACM at the system level will be best represented by the monitoring of the mass flow at the PACK outlet rather than the temperature. It

would also seem that the ACM would have to be removed for maintenance without knowing the exact cause of degradation.

Interpreting the results at the component level, it is evident that there exists a strong synergy between the results acquired under mechanical efficiency degradation and the turbine efficiency degradation. This stems from the fact that in both cases the power that can be delivered to the compressor substantially reduces, in the case of mechanical efficiency degradation the power produced by the turbine is lost due to the presence of mechanical losses associated with the interconnecting shaft. In the case of turbine efficiency degradation the turbine's ability to produce power substantially reduces with increase in the severity level. Both fault modes, although stemming from two different sources have the same effect on the PACK performance characteristics both at the component and system levels. From the ACM fault diagnostics perspective, based on the three fault modes evaluated in this study, it can be concluded that the PACK outlet mass flow, parameter can best capture the degradation in the PACK ACM, rather than the temperature.

Based on the the findings conceived from the evaluation of degradation in the PACK primary heat exchanger, secondary heat exchanger, ram inlet, TCV, and PV reported by the authors in [8,9], and with the results reported herein for the ACM. The formulation of arobust PACK system-level diagnostics can be implemented to formulate a through-life maintenance approach for the PACK, like the one demonstrated by the authors in Ref. [10] for an aircraft auxiliary power unit. In addition, the results acquired for the fault simulation of the PACK components at the system level can be readily implemented within the aircraft-level reasoning framework reported by the authors in Ref. [20] to facilitate the scientific understanding of how the PACK component level faults interact with the other aircraft systems i.e., APU, engines, and electrical power. The results reported in this study, therefore, make an important contribution towards enabling the formulation of PACK diagnostics at the system level, as well as the potential to facilitate reasoning of PACK component faults at the aircraft level.

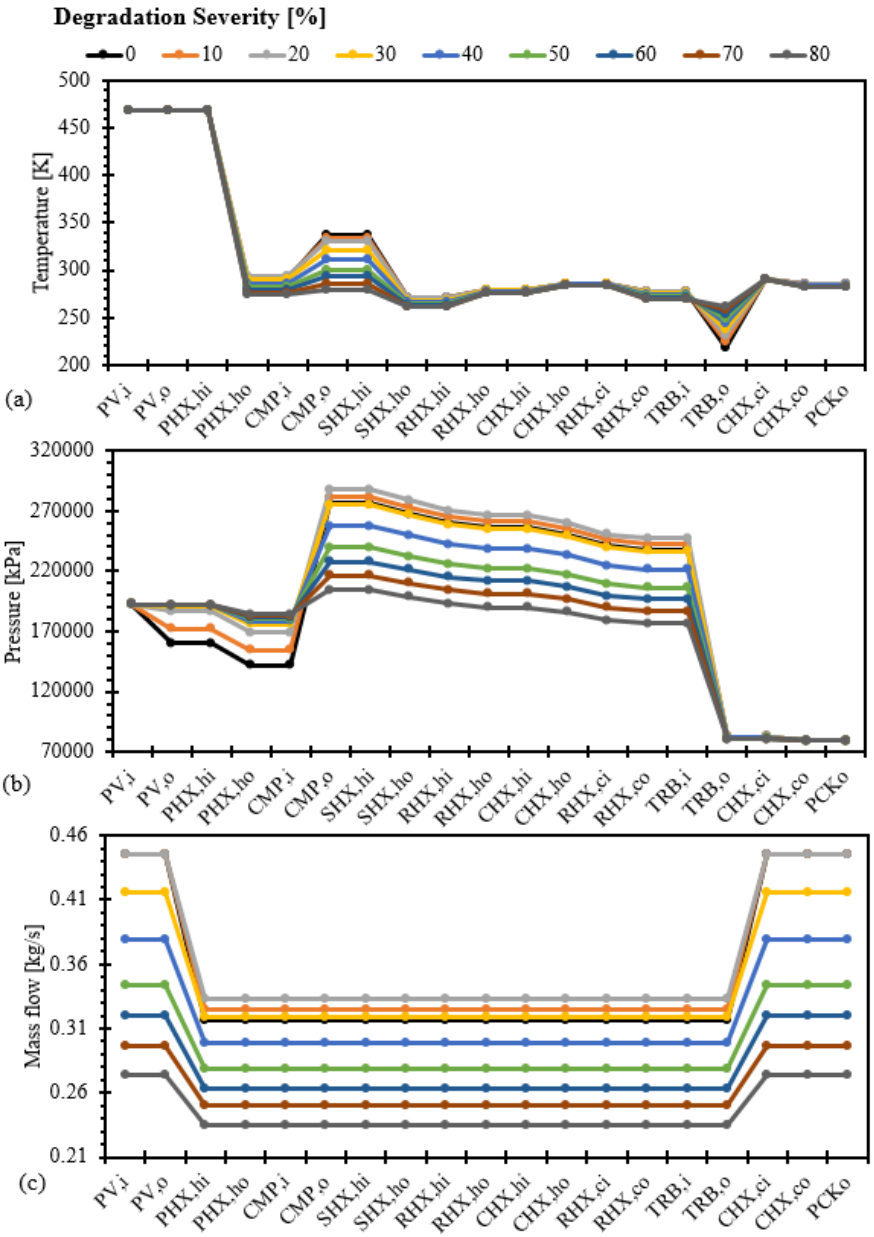

Figure 7: Turbine efficiency degradation results under various severities. 0% and 80 % represents healthy Severely degraded.

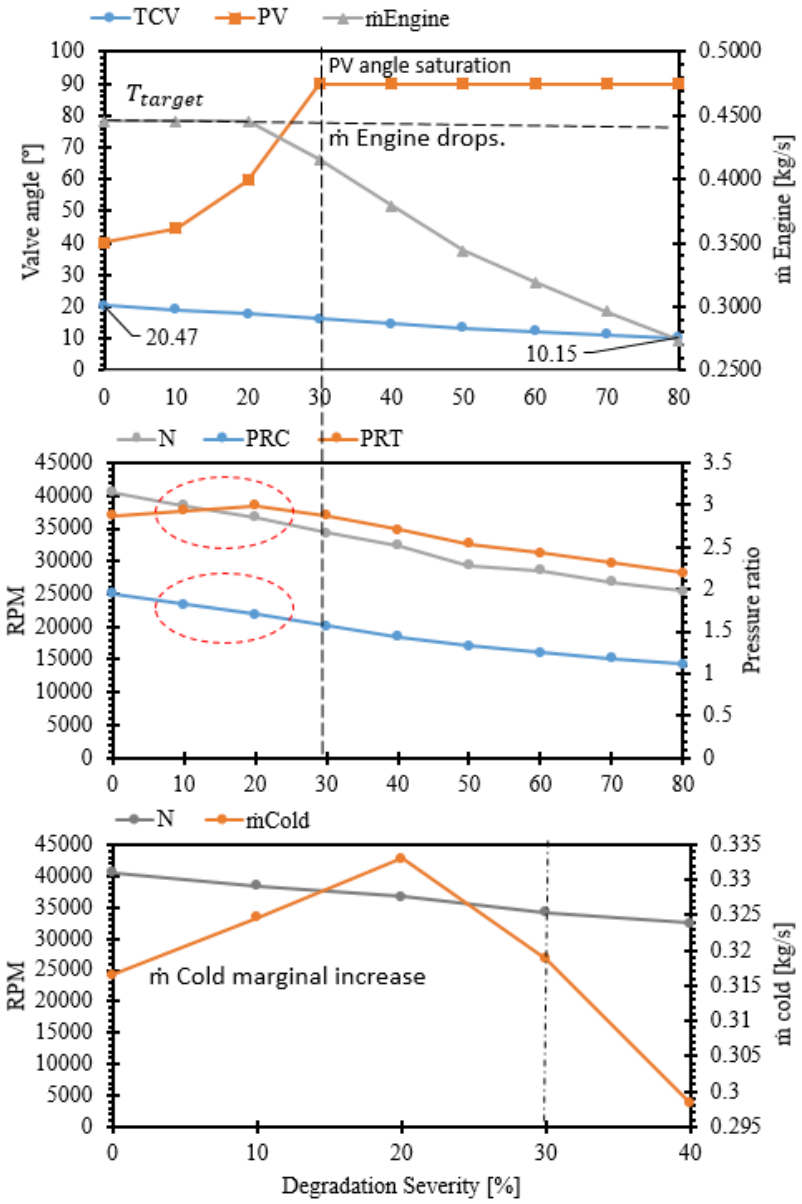

Figure 8: Turbine efficiency degradation results under various severities.

4 Summary and Conclusions

The ACM plays a pivotal role in enabling the aircraft ECS to supply conditioned air in order to ensure the comfort and safety of the passengers. In this paper, a robust, cost-effective, and computationally efficient aircraft ECS simulation framework has been implemented to evaluate critical faults modes of the ACM at both component and system levels. The overall evaluation includes a qualitative and quantitative assessment of the fault modes such as fouling in the compressor and turbine, and the mechanical losses associated with the interconnecting shaft. The acquired results are presented in terms of temperature, pressure, and mass flow throughout the PACK. The interpretation of the results describes the engineering and physics of the PACK when subjected to faults in the ACM under various degradation severities at the system level.

From the fault diagnostics point of view, the key learning point is that there is no underlying difference between how the PACK responds in terms of engineering and physics when subjected to degradation in mechanical efficiency, compressor efficiency, and turbine efficiency. The acquired results suggest that, for all three fault modes, the PV controller can compensate for the degradation severity of up to 20%, allowing the PACK to sustain the delivery of demanded temperature and mass flow. For degradation severity beyond 20%, the PACK can deliver the demanded temperature with a reduced mass flow. This significantly affects the PACK's ability to meet the cabin demand. The acquired results demonstrated that, from the ACM fault diagnostics perspective, the parameter that best captures the degradation in the PACK ACM can be represented by monitoring the PACK outlet mass flow, rather than the temperature. The acquired results, therefore, make an important contribution towards enabling the formulation of PACK diagnostics at the system level, as well as the potential to facilitate reasoning of the PACK component faults at the aircraft level.

Acknowledgements

The Boeing Company, as part of their collaboration with Cranfield University's IVHM Centre, funded this work; the authors would like to thank them for their support of this project.

Conflict of Interest

There is no conflict of interest.

References

1. Peggy, Hollinger, “Smarter aircraft create a wealth of data but it remains underexploited.” Finanancial Times. June 12, 2015. www.ft.com/content/3f956a92-0943-11e5-b643-00144feabdc0.
2. Derek, Costanza, Brian, Prentice., “Recover and Rebuild - Toward a Leaner, More Agile MRO Industry.”, Oliver Wyman. 2021. https://www.oliverwyman.com/our-expertise/insights/2021/apr/mro-maintenance-repair-overhaul-survey-2021.html.
3. Alexander, Grous, “Evaluating the economic benefits.”, Sky High Economics. London School of Economics. 2018. https://www.lse.ac.uk/business/consulting/assets/documents/sky-high-economics-chapter-two-evaluating-the-economic-benefits.pdf.
4. Esperon, M., Philip, J., Jennions, I., 2013 “A review of Integrated Vehicle Health Management tools for legacy platforms: Challenges and opportunities”., Journal of Progress in Aerospace Sciences, 56, pp.19-34.
5. American Society of Heating Refrigerating and Air-Conditioning Engineers, 2011 ASHRAE Handbook - HVAC Applications. 2011.
6. Jennions, I., Ali, F., Esperon, M., Escobar, I., 2020 “Simulation of an aircraft environmental control system”., Appl. Thermal. Eng. 172, pp. 1125-1139.
7. Liu, C., Sun, F., Wang, S.N., XU, G., 2020 “Bayesian network method for fault diagnosis of civil aircraft environment control system” Proc. Inst. Mech. Eng. Part I Journal of System Control Engineering, Vol. 234, Issue 5, pp. 662–674, doi: 10.1177/0959651819884747.
8. Jennions, I., Ali, F., 2021, “Assessment of Heat Exchanger Degradation in a Boeing 737-800 Environmental Control System,” ASME J Therm Sci Eng Appl, 13(6), pp. 155 – 168.
9. Chowdhury, S., Ali, F., Jennions, I., 2022 “Boeing 737-400 Passenger Air Conditioner Control System Model for Accurate Fault Simulation,” ASME, J Therm Sci Eng Appl, 14(9), September 2022.
10. Skliros, C., Ali, F., Jennions, I., 2022 “Aircraft Systems Level Diagnosis with Empasis on maintenance Decisions. Proc. Inst. Mech. Eng. Part O: Journal of Risk and Reliability, Volume 236, Issue 6, Pages 1057-1077.
11. Boeing 737-300/400/500 Aircraft Maintenance Manual, D6-37580.
12. Aeronautics Guide, 2022: Aircraft Air Conditioning System: available at: https://www.aircraftsystemstech.com/2017/05/aircraft-air-conditioning-systems.html.
13. Santos, P., Andrade, C., Zaparoli, E., 2014 “A Thermodynamic Study of Air Cycle Machine for Aeronautical Applications” International Journal of Thermodynamics, Vol. 17(3), pp.117 -126.
14. Smith, A., Childs, T., Chen, R., 2018 “Study into Electrically Shaft Driven Air Cycle Machine”, 1st International Conference on Advances in Aerospace Structures, Systems and TechnologyAt: Croydon, London, United Kingdom.
15. Kruz, R., Brun, K., Wollie, M., 2009 “Degradation effects on industrial gas turbines”ASME J Eng. Gas Turbines Power, 131: 062401, https://doi.org/10.1115/1.3097135.
16. Graf, M. B., Wong, T. S., Greitzer, E.M., MArble, F.E., Tan, C.S., Shin, H.W., Wisler, D.C., 1998 “Effects of non- Axisymmetric tip clearance on axial compressor performance and stability” ASME J. Turbomach, 120(4): 648-661, https://doi.org/10.1115/1.2841774.
17. Igie, u., Pilidis, P., Fouflias, D., Ramsden, K., Laskaridis, P., 2014 “Industrial Gas Turbine Performance: Compressor Fouling and On-Line Washing” ASME J. Turbomach. Oct 2014, 136(10), https://doi.org/10.1115/1.4027747.
18. Zwebek, I., Pilidis, P., 2014 “Degradation effects on combined cycle power plant performance -part III: Gas and steam turbine component degradation effects,”ASME J. Eng. Gas Turbines Power, vol. 126, no. 2, pp. 306–315.
19. Boyle, J. R., 1994 “Prediction of surface roughness and incidence effects on turbine

performance," ASME J. Turbomach. 116(4): pp.745-751.
20. Ezhilarasu, C.M., Jennions, I,K., 2021 "Development and Implementation of a Framework for Aerospace Vehicle Reasoning" IEEE Access, Volume: 9, pp.108028-108048, 10.1109/ACCESS.2021.3100865.

List of Figures

Evaluation of component level degradation in the Boeing 737-800 air cycle machine

Jennions, Ian

2022-12-19

Jennions IK, Ali F. (2023) Evaluation of component level degradation in the Boeing 737-800 air cycle machine. Journal of Thermal Science and Engineering Applications, Volume 15, Issue 3, March 2023, Article number 031014, Paper number TSEA-22-1375

https://doi.org/10.1115/1.4056510